BASIC RESEARCH PAPERS

Effect of exercise on hemodynamic conditions in the abdominal aorta

Charles A. Taylor, PhD, Thomas J.R. Hughes, PhD, and **Christopher K. Zarins, MD,** *Stanford, Calif*

Purpose: **The beneficial effect of exercise in the retardation of the progression of cardiovascular disease is hypothesized to be caused, at least in part, by the elimination of adverse hemodynamic conditions, including flow recirculation and low wall shear stress. In vitro and in vivo investigations have provided qualitative and limited quantitative information on flow patterns in the abdominal aorta and on the effect of exercise on the elimination of adverse hemodynamic conditions. We used computational fluid mechanics methods to examine the effects of simulated exercise on hemodynamic conditions in an idealized model of the human abdominal aorta.**

Methods: **A three-dimensional computer model of a healthy human abdominal aorta was created to simulate pulsatile aortic blood flow under conditions of rest and graded exercise. Flow velocity patterns and wall shear stress were computed in the lesion-prone infrarenal aorta, and the effects of exercise were determined.**

Results: **A recirculation zone was observed to form along the posterior wall of the aorta immediately distal to the renal vessels under resting conditions. Low time-averaged wall shear stress was present in this location, along the posterior wall opposite the superior mesenteric artery and along the anterior wall between the superior and inferior mesenteric arteries. Shear stress temporal oscillations, as measured with an oscillatory shear index, were elevated in these regions. Under simulated light exercise conditions, a region of low wall shear stress and high oscillatory shear index remained along the posterior wall immediately distal to the renal arteries. Under simulated moderate exercise conditions, all the regions of low wall shear stress and high oscillatory shear index were eliminated.**

Conclusion: **This numeric investigation provided detailed quantitative data on the effect of exercise on hemodynamic conditions in the abdominal aorta. Our results indicated that moderate levels of lower limb exercise are necessary to eliminate the flow reversal and regions of low wall shear stress in the abdominal aorta that exist under resting conditions. The lack of flow reversal and increased wall shear stress during exercise suggest a mechanism by which exercise may promote arterial health, namely with the elimination of adverse hemodynamic conditions. (J Vasc Surg 1999;29:1077-89.)**

Exercise has numerous overall health benefits. Exercise improves cardiorespiratory fitness levels and lowers all-cause and cardiovascular mortality rates.[1-5] The fitness benefits of exercise include increased cardiovascular functional capacity, increased maximal cardiac output, increased extraction of oxygen from the blood, and decreased myocardial oxygen demand.[5] Recent studies have noted that increased fitness levels, as measured with maximal exercise treadmill tests, can result in up to a three-fold decrease in mortality rate.[3]

In spite of the numerous studies on the overall benefits of exercise, the mechanism by which exercise improves arterial health and the intensity and duration of exercise needed to achieve benefit have not been determined. It is postulated that the mechanism by which exercise reduces vascular disease is a result of direct and indirect causes. *Direct causes* are those that occur while exercise is being performed and end on the cessation of exercise. Hemodynamic factors, such as increased shear stresses and removal of lipid

From the Division of Vascular Surgery (Drs Taylor and Zarins), Department of Surgery, and the Division of Mechanics and Computation (Drs Taylor and Hughes), Department of Mechanical Engineering, Stanford University.

Reprint requests: Dr Charles A. Taylor, Assistant Professor, Division of Vascular Surgery, Stanford University Medical Center, Suite H3600, Stanford, CA 94305-5450.

0741-5214/99/$8.00 + 0 **24/1/96862**

molecules from the vessel luminal surface, are examples of potential direct mechanisms by which exercise reduces vascular disease. Increased shear stress increases nitric oxide and prostacyclin release and inhibits atherosclerotic processes.[6] *Indirect causes* would be triggered by the onset of exercise and would presumably continue on cessation of exercise. These causes would, in general, be systemic and unrelated to the local changes in the hemodynamic environment. The effect that exercise has on controlling lipid abnormalities, diabetes, and obesity, on lowering blood pressure, on altering lipid and carbohydrate metabolism, and on increasing high-density lipoproteins would be examples of indirect mechanisms by which exercise reduces vascular disease.

Recommendations on exercise intensity and duration have traditionally been made on the basis of improving cardiorespiratory fitness. In the American College of Sports Medicine's (ACSM) 1990 position stand on exercise, it was recommended that, to develop and maintain cardiorespiratory fitness, adults should train 3 to 5 days per week at 60% to 90% of maximum heart rate (HR_{max}) or at 50% to 85% of maximum oxygen uptake for 20 to 60 minutes with large muscle groups (eg, lower limb exercise, such as running and bicycling).[1] The levels of exercise were categorized after Pollack and Wilmore[7] in the following manner: *very light exercise* was defined as less than 35% of HR_{max}, *light exercise* was defined as 35% to 59% of HR_{max}, *moderate exercise* was defined as 60% to 79% of HR_{max}, *heavy exercise* was defined as 80% to 89% of HR_{max}, and *very heavy exercise* was defined as more than 90% of HR_{max}. Clearly, the recommendations of the ACSM 1990 position stand reflect moderate to heavy exercise conditions.

The ACSM recommendation distinguished between exercise for fitness (the ability to perform moderate to vigorous levels of physical activity without undue fatigue and the capability of maintaining such activity throughout life) and the effect of exercise on the reduction of cardiovascular disease. It was noted that "…lower levels of physical activity than recommended by this position statement may reduce the risk for certain chronic degenerative diseases and yet may not be of sufficient quantity or quality to improve maximum oxygen uptake."[1] Recent public health recommendations have reinforced this view that, for overall health benefits, individuals should engage in, at the least, moderate levels of physical activity in lieu of a regular exercise program.[2]

In addition to causing systemic changes in the cardiovascular system, exercise conditions have a local effect on blood flow in the major arteries. For example, in vivo and in vitro models have shown that the hemodynamics of the infrarenal abdominal aorta are characterized by regions of complex recirculating flow under resting conditions[8-15] and further that these regions of flow recirculation are not observed under lower limb exercise conditions.[16-18] Clearly, to examine the effect of graded exercise on hemodynamic conditions in the abdominal aorta, detailed quantitative data on flow conditions are necessary.

In recent years, computational techniques have been used increasingly by researchers who seek to understand vascular hemodynamics.[19-24] These methods can augment the data provided by in vitro and in vivo methods by enabling a complete characterization of hemodynamic conditions under precisely controlled conditions. In contrast to the relatively large number of studies of pulsatile flow in models of the carotid bifurcation and end-to-side anastomosis, there have been few numeric studies of flow in the abdominal aorta. Taylor et al[25] described the flow in an abdominal aorta model under simulated resting and exercise steady flow conditions. It was noted that a region of flow recirculation and low wall shear stress develops along the posterior wall of the infrarenal abdominal aorta under simulated resting conditions and disappears under simulated exercise conditions. Taylor et al[26,27] described, qualitatively, the pulsatile flow in a model of an abdominal aorta under simulated resting and exercise conditions. As in the steady flow case, a flow recirculation region was noted at mid diastole in the infrarenal abdominal aorta under simulated resting conditions and disappeared under exercise conditions. Taylor et al[28] detailed, quantitatively, the hemodynamic conditions under simulated resting pulsatile flow conditions in an idealized model of an abdominal aorta. The flow velocity patterns and spatial variations of mean wall shear stress and oscillatory shear index were reported.

The computational method described herein was used to quantitatively characterize the hemodynamic conditions under simulated resting, light exercise, and moderate exercise pulsatile flow conditions in an idealized model of an abdominal aorta. The changes in the flow velocity field, the spatial variations of wall shear stress, and the temporal oscillations of wall shear stress were described in detail, and the effect of exercise on abdominal aorta hemodynamics was determined. We tested the hypothesis that simulated lower limb exercise eliminates hemodynamic conditions, such as flow recirculation, low mean wall shear stress, and temporal oscillations in shear stress, that are thought to be responsible for the localization of vascular disease in the infrarenal abdominal aorta.[15,28]

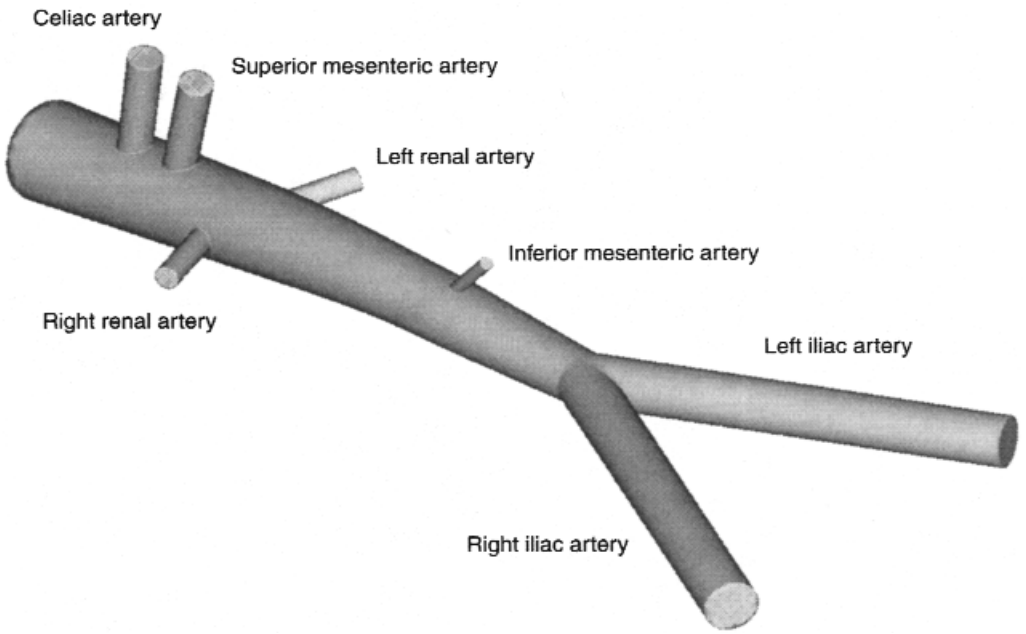

Fig 1. Abdominal aorta model with branches identified.

Further, we tested the hypothesis that light exercise conditions are sufficient to eliminate regions of low mean shear stress and high oscillatory shear index in the infrarenal abdominal aorta.

METHODS

A geometric solid model of an idealized abdominal aorta, shown in Fig 1, was constructed with a custom software system, "The Stanford Virtual Vascular Laboratory," which was developed to aid in the solution of blood flow problems.[26,27] This system was developed with a knowledge-based, object-oriented programming language and combines geometric solid modeling, automatic finite element mesh generation, multiphysics finite element methods, and scientific visualization capabilities.[29-33] The anatomic dimensions of the idealized abdominal aorta model were obtained from Moore et al.[10] The model constructed is not symmetric about the midsagittal plane but rather includes the feature that the left renal artery is located inferior to the right renal artery. A finite element mesh with 268,563 tetrahedral elements and 58,151 nodes was generated with an automatic mesh generator.[29]

Approximately 70% of the blood that enters the abdominal aorta under resting conditions is extracted by the celiac, superior mesenteric, and renal arteries. Most of the remaining 30% flows down the infrarenal segment through the bifurcation into the legs. Under lower limb exercise conditions, the total abdominal aorta flow increases and, in addition, the amount of blood extracted by the celiac, superior mesenteric, and renal arteries decreases, which further increases the infrarenal blood flow.[34] The flow conditions are summarized in Table I, and the mean flow distribution is given in Table II. The values for resting and moderate exercise conditions were obtained from Moore et al,[10] and light exercise conditions were taken to be midway between these two states.

Table I. Flow conditions

	Resting	*Light exercise*	*Moderate exercise*
Cardiac output (L/min)	4.5	6.0	7.5
Heart rate (bpm)	66	100	133
Abdominal aorta flow (L/min)	2.7	4.1	5.6

In contrast to steady flow studies, in vitro and computational studies of pulsatile blood flow necessitate the specification of flow waveforms and of mean flow rates. The flow rates as a function of time used in the present study for the inflow and branch vessels are shown in Fig 2. The flow rate waveforms shown in Fig 2 for the renal artery and iliac artery are those for each of the right and left renal and iliac arteries, respectively. The suprarenal and infrarenal flow rate time functions and the celiac, superior mesenteric, renal, and inferior mesenteric mean flow rates were obtained from Moore and Ku.[14,16] The

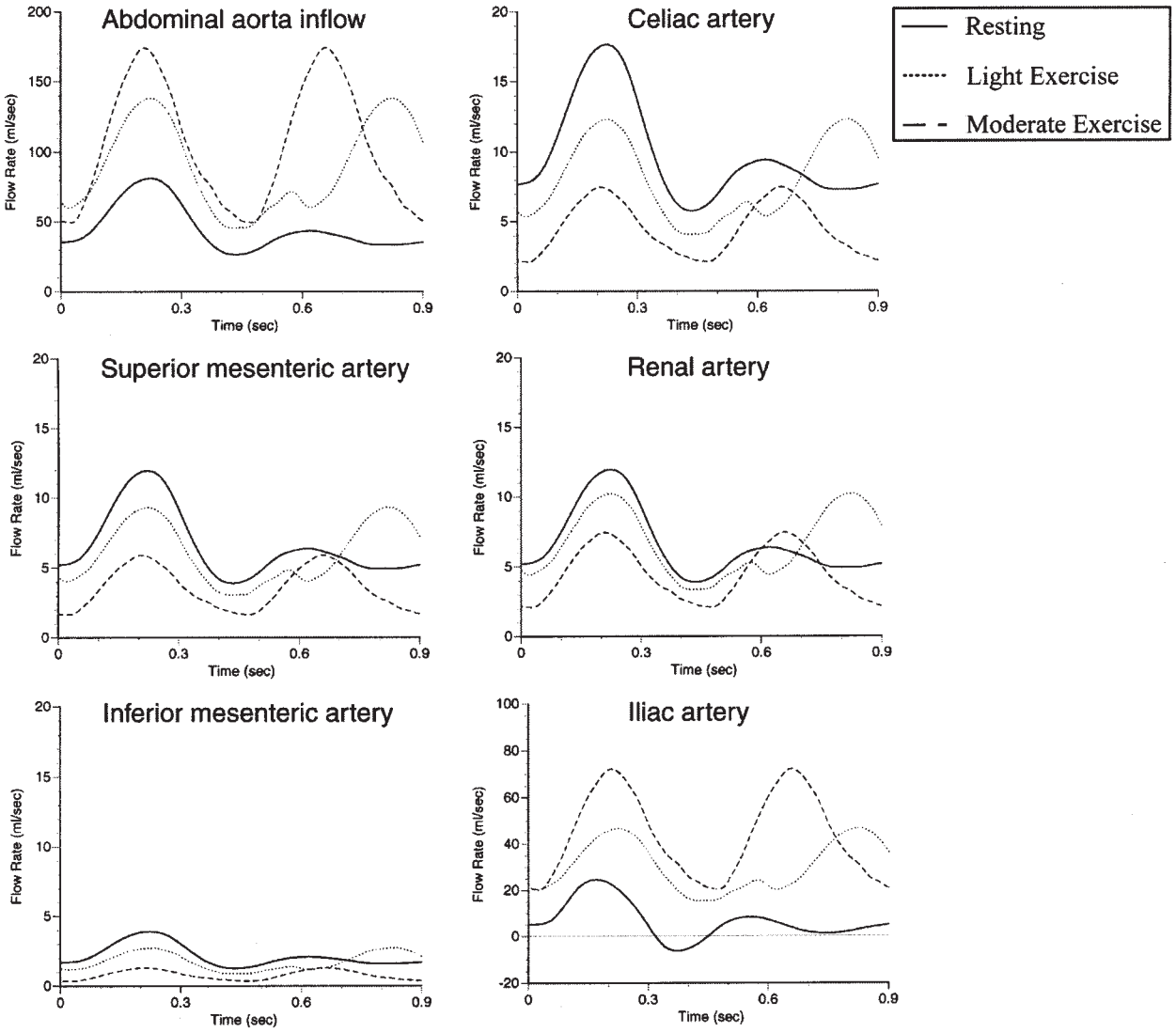

Fig 2. Flow rate time functions. Note ordinate scales for each plot.

Table II. Mean flow distribution (L/min)

Artery	*Resting*	*Light exercise*	*Moderate exercise*
Celiac	0.53	0.41	0.28
Superior mesenteric	0.4	0.31	0.22
Left renal	0.4	0.34	0.28
Right renal	0.4	0.34	0.28
Inferior mesenteric	0.13	0.09	0.06
Left iliac	0.4	1.32	2.25
Right iliac	0.4	1.32	2.25

flow rate waveforms in the celiac, superior mesenteric, renal, and inferior mesenteric arteries were computed to conserve mass and yield the mean flow rates given in Table II. Note that, under resting and exercise conditions, the abdominal aorta inflow and renal artery outflows are always positive, whereas under resting conditions, the iliac flow waveform exhibits the triphasic character of in vivo measurements of infrarenal aortic flow. On the basis of the volume flow waveforms shown in Fig 2, pulsatile flow velocity boundary conditions, derived from Womersley theory, were prescribed for the inflow boundary and all outflow boundaries, excluding the left and right iliac outflow boundaries, where zero pressure boundary conditions were prescribed.[35] It should be noted that the Womersley boundary conditions are time-dependent, axisymmetric velocity profiles at the inlet and outlet boundaries.

Computational modeling of blood flow necessi-

tates solving, in the general case, three-dimensional, transient flow equations in deforming blood vessels. The appropriate framework for problems of this type is the arbitrary Lagrangian-Eulerian (ALE) description of continuous media in which the fluid and solid domains are allowed to move to follow the distensible vessels and deforming fluid domain.[36]

The vessel diameter change during the cardiac cycle is observed to be approximately 5% to 10% in most of the major arteries, and, as a first approximation, the vessel walls are often treated as being rigid. In addition, in diseased vessels, which are often the subject of interest, the arteries are even less compliant and wall motion is further reduced. The assumption of zero wall motion was used for the computations presented herein. Under this assumption, the Lagrangian-Eulerian description of incompressible flow in a deforming fluid domain reduced to the Eulerian description of a fixed spatial domain.

The strong form of the problem governing incompressible, Newtonian fluid flow in a fixed domain consists of the Navier-Stokes equations and suitable initial and boundary conditions. Direct, analytic solutions of these equations are not available for complex domains, and numeric methods must be used. The finite element method has been the most widely used numeric method for solving the equations governing blood flow.[37]

The finite element method used in the present investigation is based on the theory of stabilized finite element methods developed by Brooks and Hughes[38] and Hughes et al.[39] The method is described in detail by Taylor et al[27,28] as it is implemented in the commercial finite element program, Spectrum.[32] The basic idea is to augment the Galerkin finite element formulation with a least-squares form of the residual, including appropriate stabilization parameters. These stabilization parameters are designed so that the method achieves exact solutions in the case of one-dimensional model problems that involve, for example, the steady advection-diffusion equation. A semidiscrete formulation with a second-order accurate time-stepping algorithm is used, which results in a nonlinear algebraic problem in each time step. This nonlinear problem is linearized, and the resulting linear systems of equations are iteratively solved with conjugate gradient and matrix-free Generalized Minimal Residual solvers to reduce memory requirements.[40] Because the flow computations were performed on a parallel computer, the computational domain was divided into 16 subdomains with a graph partitioning method.[41] The nonlinear evolution equations were solved for the velocity and pressure fields over three cardiac cycles with 200 time steps per cardiac cycle on an IBM SP-2 parallel computer (Somers, NY). The method used has been shown via analytic and experimental validation studies to yield accurate solutions for pulsatile flow problems.[27]

In addition to the velocity field, quantitative values of the magnitude of the surface tractions are also of interest. The traction vector (t) can be computed from the stress tensor (δ) and surface normal vector (n) by the equation, $t = \delta n$, and then the *surface traction vector* (t_s), defined as the tangential component of the traction vector, can be computed from $t_s = t - (t \cdot n)n$.

We can define the *mean shear stress* (τ_{mean}), a scalar quantity, as the magnitude of the time-averaged surface traction vector as

$$\tau_{mean} = \left| \frac{1}{T} \int_0^1 t_s dt \right|$$

and define the *absolute shear stress* (τ_{abs}), another scalar quantity, as the time-averaged magnitude of the surface traction vector as

$$\tau_{abs} = \frac{1}{T} \int_0^1 \left| t_s \right| dt$$

After He and Ku,[42] we define the oscillatory shear index (OSI) as

$$OSI = \frac{1}{2} \left(1 - \frac{\tau_{mean}}{\tau_{abs}} \right)$$

Note that the surface traction is a vector quantity and thus includes the direction of the surface force and its magnitude. The magnitude of the surface traction reduces to the wall shear stress, $\tau_w = 4\mu Q/\pi r^3$, where μ is the viscosity, Q is the flow rate, and r is the lumen radius, in the special case of the steady, uniaxial flow of a Newtonian fluid in a circular cylinder. However, for complex, recirculating, and time-dependent flow fields, such as those that occur in the abdominal aorta, the surface traction is a more general and useful measure of surface forces than the relation for wall shear stress, τ_w, given previously.

RESULTS

A contour slice of axial velocity and a vector slice of the velocity field are displayed in Fig 3 under simulated resting, light exercise, and moderate exercise conditions at four times in the cardiac cycle along the midsagittal plane of the aorta. Note that under resting conditions a vortex developed along the posterior wall of the aorta. Under light exercise conditions, this flow recirculation region, while still apparent, had been reduced substantially in size. Under

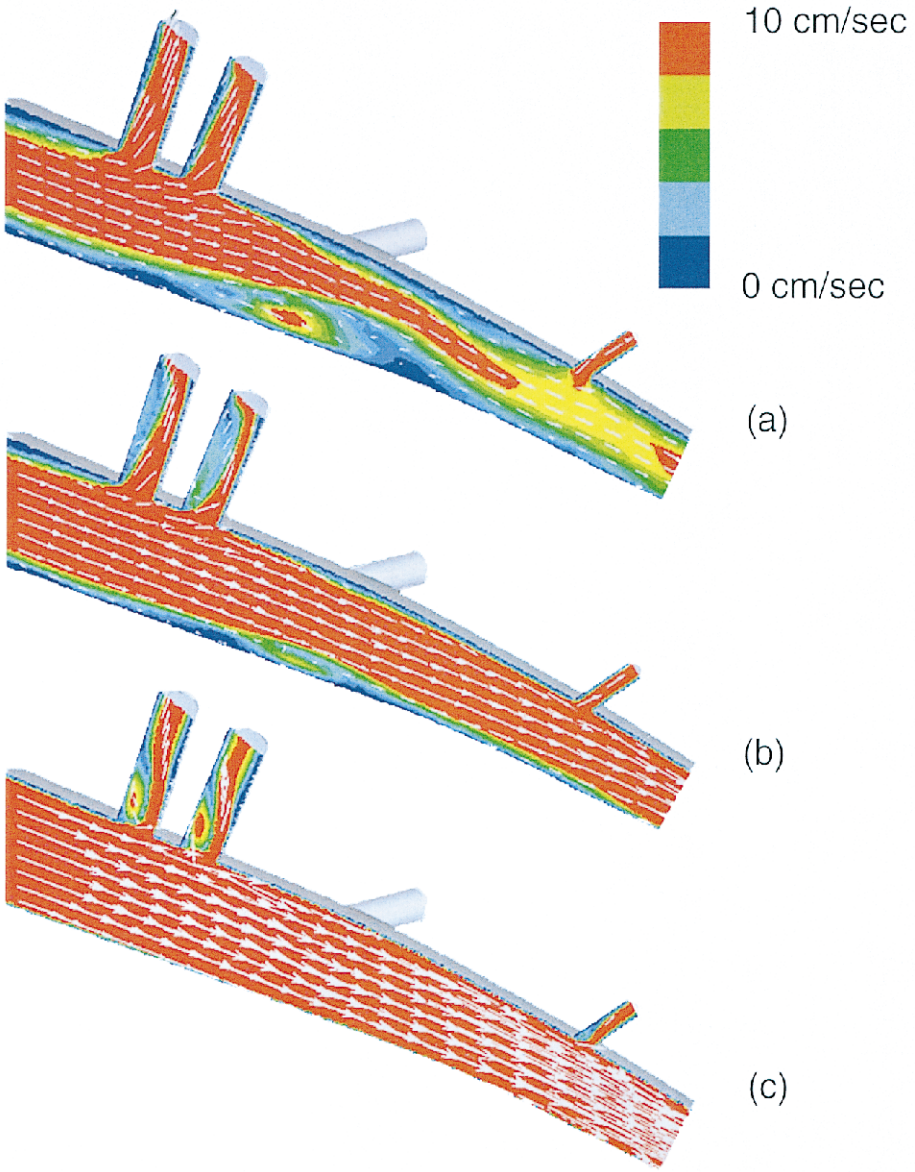

Fig 3. Midplane slice of abdominal aorta model that displays contours of axial velocity and velocity vector field for *(a)* resting conditions, *(b)* light exercise conditions, and *(c)* moderate exercise conditions.

moderate exercise conditions, this flow recirculation region was absent.

Contour plots of time-averaged (mean) wall shear stress are displayed in Fig 4 along the posterior wall. Note that under resting conditions, regions of low (<1 dyne/cm^2) mean wall shear stress were apparent along the posterior wall opposite the celiac and superior mesenteric arteries and below the renal artery branches along the lateral and posterior walls. Under light exercise conditions, a single region of low mean wall shear stress was observed along the posterior wall at the level of the renal arteries. No regions of low mean wall shear stress were apparent under moderate exercise conditions.

Mean wall shear stress is plotted as a function of arc length in Figs 5 and 6 along the anterior and posterior walls, respectively. It was noted that, along the anterior wall, gaps in the plots of shear stress corresponded to the location of the branch vessels. It was also observed that mean shear stress increased significantly in the neighborhood of the celiac, superior mesenteric, and inferior mesenteric vessels.

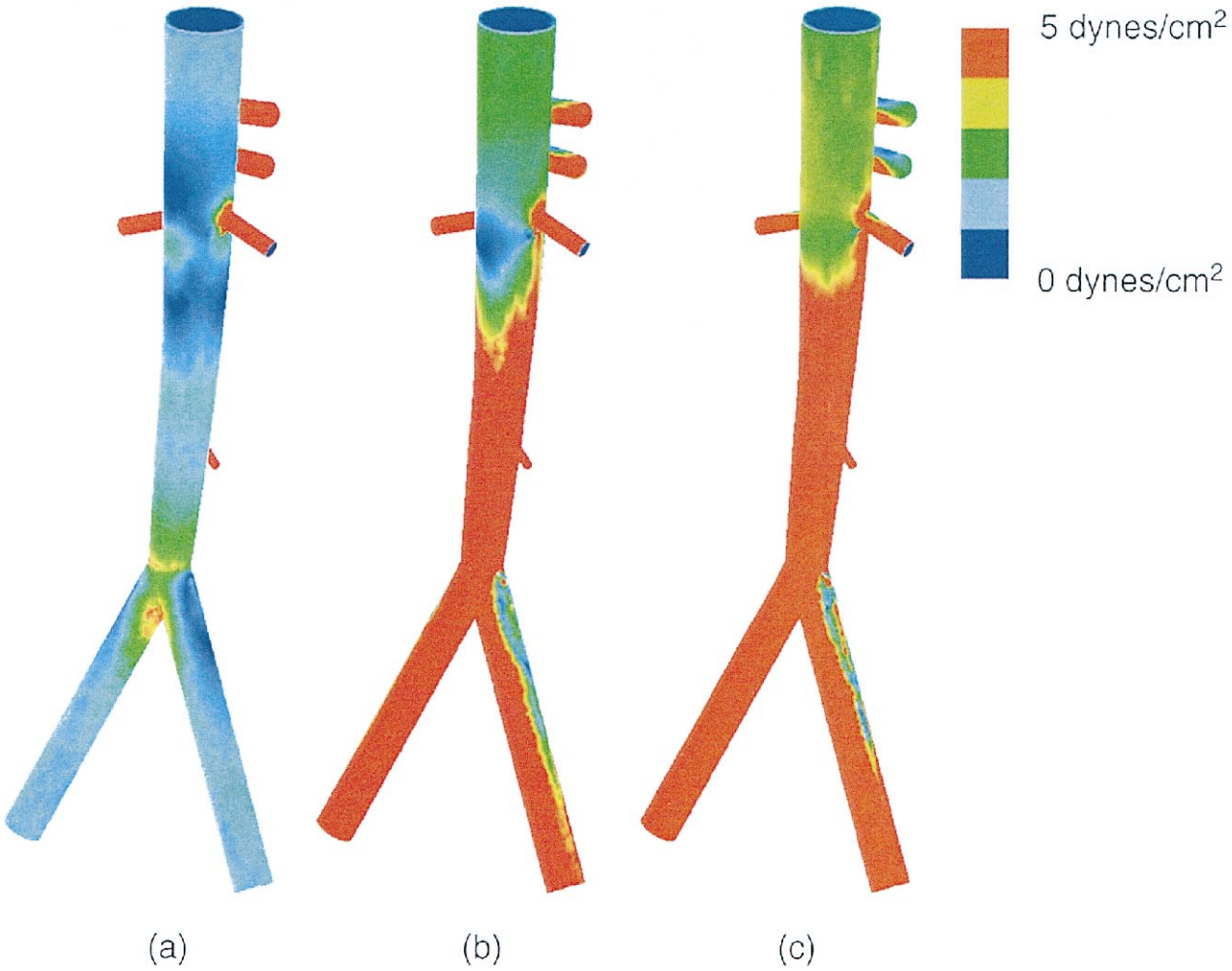

Fig 4. Mean shear stresses for abdominal aorta model under *(a)* resting conditions, *(b)* light exercise conditions, and *(c)* moderate exercise conditions.

Under resting, light exercise, and moderate exercise conditions, the mean shear stress along the anterior wall in the distal infrarenal aorta exceeded the shear stress at the level of the diaphragm. It was observed that under resting conditions the mean shear stress approached zero along the posterior wall opposite the celiac and superior mesenteric vessels and approximately 2 cm distal to the left renal artery. Under light exercise conditions, a single region of low mean wall shear stress appeared immediately distal to the left renal artery. Under moderate exercise conditions, no regions of low mean wall shear stress were observed along the posterior wall of the abdominal aorta. It was also observed that under all flow conditions the mean shear stresses increased in the distal infrarenal abdominal aorta to a level that exceeded that at the level of the diaphragm.

The OSI is plotted as a function of arc length in Figs 7 and 8 along the anterior and posterior walls, respectively. Examination of the OSI along the anterior wall under resting conditions revealed a sharp increase of the OSI from zero in the suprarenal aorta to approximately 0.3 immediately distal to the left renal artery and then a gradual decline to a value of approximately 0.05 at the level of the aortic bifurcation. Under light exercise conditions, the OSI was zero along the anterior wall except for immediately distal to the left renal artery where it increased from zero to approximately 0.05. Under moderate exercise conditions, the OSI was zero along the anterior wall of the abdominal aorta. The OSI along the posterior wall under resting conditions increased from zero in the suprarenal aorta to approximately 0.4 opposite the superior mesenteric artery, decreased to less than

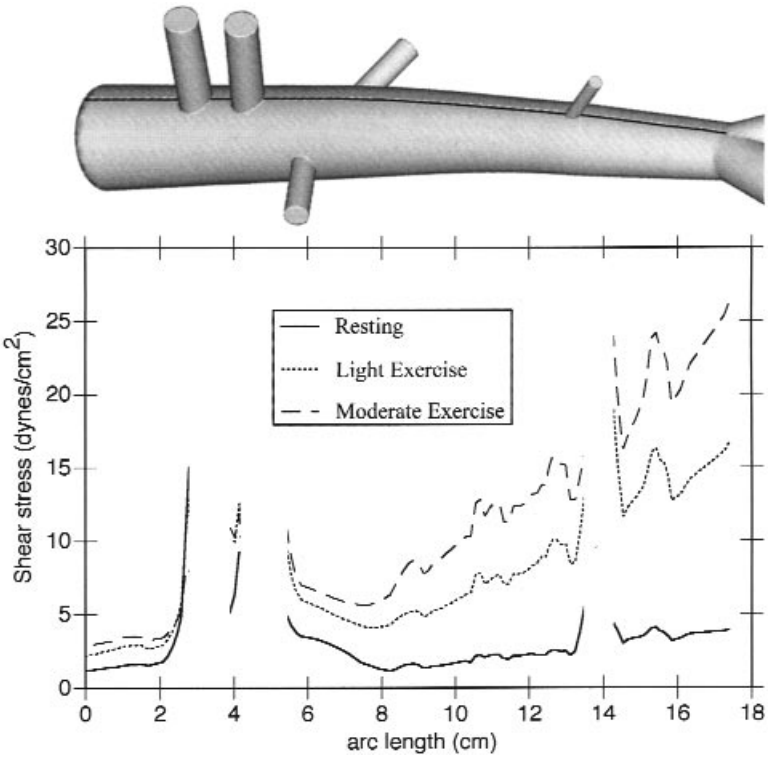

Fig 5. Mean shear stress along anterior wall from diaphragm to aortic bifurcation.

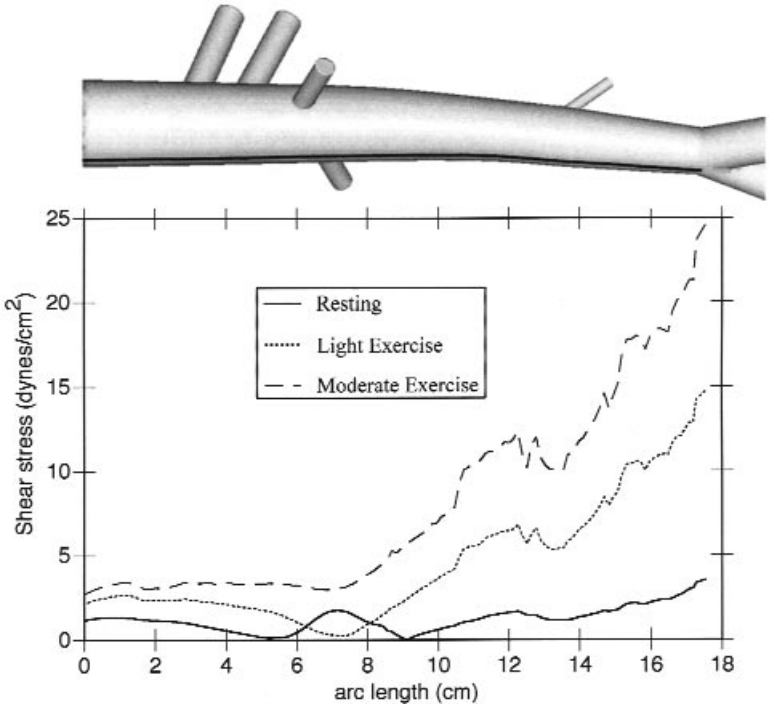

Fig 6. Mean shear stress along posterior wall from diaphram to aortic bifurcation.

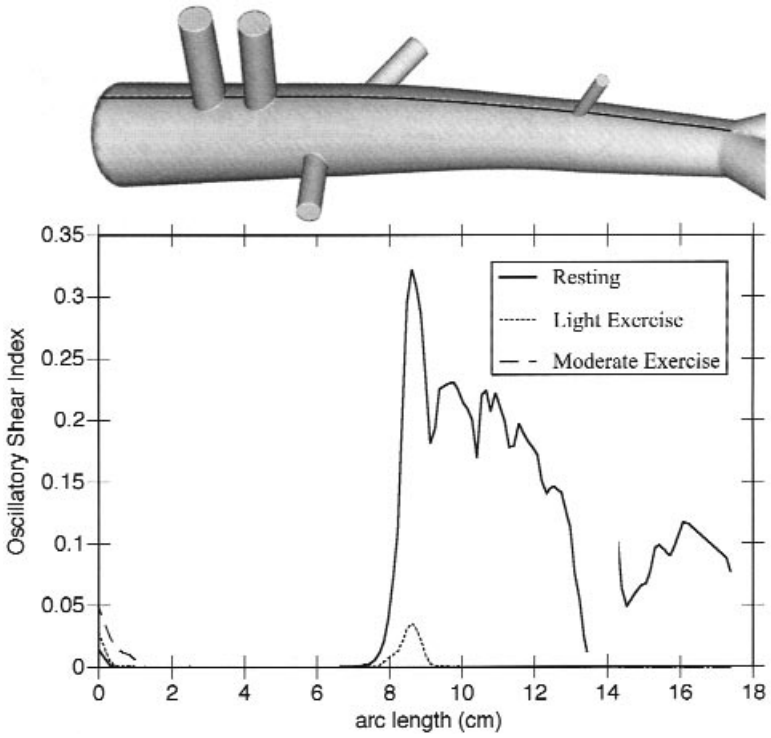

Fig 7. Oscillatory shear index along anterior wall from diaphragm to aortic bifurcation.

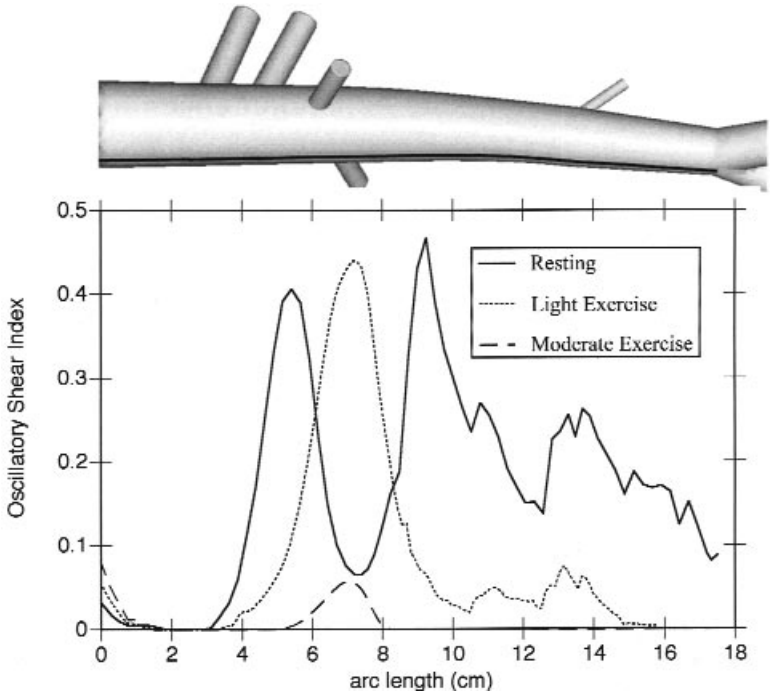

Fig 8. Oscillatory shear index along posterior wall from diaphragm to aortic bifurcation.

0.1 at the level of the renal arteries, increased to a maximum value of 0.47 distal to the renal arteries, and then decreased to a value of approximately 0.1 at the level of the aortic bifurcation. Under light exercise conditions, the OSI along the posterior wall increased from zero in the suprarenal aorta to approximately 0.45 at the level of the the left renal artery and then decreased to less than 0.1 for the remainder of the infrarenal abdominal aorta. Under moderate exercise conditions, the OSI was zero along the posterior wall of the abdominal aorta except for immediately distal to the renal arteries where it attained a value of approximately 0.05.

DISCUSSION

The numeric method used to characterize abdominal aorta hemodynamics enables the extraction of complete spatial and temporal variations in field quantities, including velocity and shear stress, to quantitatively test hypotheses related to the effect of exercise on hemodynamic conditions. The significance of the findings regarding the effect of exercise on the velocity field and shear stresses is described subsequently, followed by an examination of the assumptions used in the present investigation.

Under resting conditions, a flow recirculation region appeared along the posterior wall of the abdominal aorta in late systole and was present throughout diastole. This recirculation region extended from the level of the renal arteries to the inferior mesenteric artery. This finding is consistent with prior in vitro[9,10,14] and in vivo[8,11,18] studies of flow in the abdominal aorta. It should be noted, however, that the extent of the flow recirculation region under resting conditions has not been reported previously because velocity measurements in the infrarenal aorta have been restricted to, at most, a few cross sections.

The plots of shear stress and oscillatory shear index along the anterior and posterior walls provide quantitative data on the spatial variation of shear down the length of the abdominal aorta. Under resting conditions, the mean shear stress in the abdominal aorta at the level of the diaphragm was calculated to be approximately 1.2 dynes/cm^2. Moore et al[15] measured the shear stress at this location to be 1.3 ± 0.6 dynes/cm^2 in an in vitro study with approximately the same flow conditions and model dimensions as those used in this study. Along the anterior wall, the ostia of the celiac, superior mesenteric, and inferior mesenteric arteries are sites of relatively high mean shear stress and low oscillatory shear index for all flow conditions. As discussed subsequently, this is believed to be the result of an inadequate modeling assumption, incorporated into the idealized model, whereby the junctures between the branch vessels and the aorta are not smoothly tapered. Under resting conditions, the anterior wall of the infrarenal aorta between the superior mesenteric and inferior mesenteric arteries was a site of low shear stress and high oscillatory shear index. Under light and moderate exercise conditions, the anterior wall of the abdominal aorta experienced mean shear stresses in excess of that found at the level of the diaphragm. Along the posterior wall, under resting conditions, the mean shear stress was low and oscillatory shear index high opposite of the superior mesenteric artery and at approximately 2 cm distal to the left renal artery in the region noted for flow recirculation. The distal abdominal aorta below the inferior mesenteric artery and proximal to the bifurcation is a site of relatively high mean shear stress and moderate values of the oscillatory shear index. Under light exercise conditions, a region of low mean wall shear stress remained, yet disappeared under moderate exercise conditions. Although shear stresses were reported by Moore et al[15] for two locations in the infrarenal abdominal aorta under resting conditions, the spatial distribution of shear stress magnitude had not been quantified previously.

As noted previously, vascular disease is more prominent in the abdominal aorta as compared with the thoracic aorta. The localization of early atherosclerotic lesions was examined by Cornhill et al[43] by staining with Sudan IV and using image processing techniques to identify sudanophilic lesions in the cadaveric aortas of young accident victims. It was noted that the highest probability of occurrence of sudanophilia was associated with the inflow tracts of the celiac, superior mesenteric, renal, and inferior mesenteric ostia. In the present study, along the aortic wall, these ostia were not observed to be sites of low mean shear stress under resting or exercise flow conditions, yet regions of low mean shear stress were noted within the branch vessels. Again, note that the model does not incorporate the tapering of the branch vessels in the immediate vicinity of the ostia.

Cornhill et al[43] also noted a region of high probability of occurrence of sudanophilia along the posterolateral wall of the infrarenal aorta and along the anterior wall between the superior and inferior mesenteric arteries and concluded that these locations were not "expected to experience unusual hemodynamic stresses." The results presented herein clearly show otherwise. Namely, under resting conditions, these regions experience low mean wall shear stress and high oscillatory shear index. Finally, Cornhill et al[43] showed areas of high probability of

occurrence of sudanophilia along the posterior wall at the level of the celiac and superior mesenteric arteries. As noted previously, under resting conditions, this is also a region of low mean wall shear stress and high oscillatory shear index. Clearly, direct correlative studies need to be performed between hemodynamic conditions and plaque localization in the abdominal aorta, but the results presented herein show that under resting conditions, low mean wall shear stress and high oscillatory shear index occur in regions noted to have a high probability of occurrence of sudanophilic lesions.

The effect of exercise on the reduction of flow recirculation, the increase of wall shear stress, and the reduction of shear stress oscillations suggests one possible direct benefit of exercise—namely, the elimination of hemodynamic conditions known to correlate with the location of atherosclerotic plaques.[45-47] Further, this study shows that light exercise does not eliminate all of the regions of low wall shear stress and high oscillatory shear index. An obvious question arises as to how a relatively short duration of exercise could have a long-term effect on cardiovascular health through a direct mechanism because this mechanism would only be active for a small fraction of the entire day. It should be noted that the relationship between increased shear stress and inhibition of disease need not be a linear relationship—namely, a doubling of shear stress for a short duration could have a substantial effect. Further, the direct action of hemodynamic forces on the vessel walls could trigger biochemical phenomena, which would act even beyond the cessation of exercise. This could be a result of the relationship between increased shear stress on the endothelium and increased nitric oxide and prostacyclin release noted by Niebauer and Cooke.[6]

The major assumptions used in this investigation involve the anatomic dimensions of the model, the flow conditions, a rigid wall approximation, and Newtonian viscosity. The use of these assumptions, as for prior in vitro investigations, is believed to constitute a reasonable first approximation to the actual hemodynamic conditions in the abdominal aortas of healthy humans.

The anatomic dimensions used in the present study were on the basis of those reported by Moore et al[10] and include a tapering of the abdominal aorta and lumbar curvature. Potential limitations of this representation include a relatively abrupt change in dimensions at the branch ostia and the lack of curvature of the branch vessels. These anatomic approximations, made on the basis of a lack of available anatomic data, would likely alter local flow conditions in the neighborhood of the ostia. The importance of including branch vessel taper and curvature in aortic flow studies merits further investigation.[44]

The physiologic conditions used in the present study were on the basis of those reported by Moore et al[10] and Moore and Ku,[14,16] but they differ in that the numeric method used herein necessitates the specification of the time-varying outflow for the celiac, superior mesenteric, renal, and inferior mesenteric vessels. In contrast, only mean flow was determined and reported by Moore et al[10] and Moore and Ku[14,16] for these branch vessels. Three features of abdominal aortic flow waveforms, consistently observed in normal subjects under resting conditions, were used in the present study. First, the flow rate is observed to be positive throughout the cardiac cycle at the entrance to the abdominal aorta at the level of the diaphragm.[12,13,48] The second feature of abdominal aortic flow observed in normal subjects under resting conditions is the triphasic flow waveform in the infrarenal aorta.[12,13,48] The third feature is a positive net renal artery flow.[12,13,48,49]

The determination of appropriate boundary conditions and flow waveforms for investigations of abdominal aorta hemodynamic conditions merits further attention, especially for exercise flow conditions in which direct measurements are problematic. In the method used in the present study, assumptions are necessary for the variation in velocity at the boundaries where flow is specified. The velocity profiles at the inlet to the abdominal aorta at the level of the diaphragm and the celiac, superior mesenteric, renal, and inferior mesenteric artery outflows were specified with Womersley theory for pulsatile flow, which results in an axisymmetric velocity profile. Moore et al[13] confirmed the validity of the assumption of axisymmetric flow in the supraceliac abdominal aorta. This condition was also used in the model flow studies reported by Pedersen et al[9] and Moore and Ku.[14,16] Regarding the outflow velocity profiles, the length of the branch vessels was chosen to minimize the effect of the outlet boundary condition on the flow in the aorta. It is likely that the assumption of planar branch vessels in the vicinity of the ostia on the aorta has a greater effect on the flow conditions in the aorta than the axisymmetric outlet velocity profile, but this was not examined in the present study.

The effect of aortic compliance was not considered in the present investigation. Prior investigations of flow in deformable models have shown that, in general, the incorporation of the effect of compliance alters the magnitude of shear stress but does not change the locations of low and high shear regions. In an investigation of the effect of wall compliance

on pulsatile flow in the carotid artery bifurcation, Perktold and Rappitsch[21] described a weakly coupled fluid-structure interaction finite element method for solving for blood flow and vessel deformation. They concluded that the wall shear stress magnitude decreased by approximately 25% in the distensible model as compared with the rigid model yet that the overall effect on the velocity field was relatively minor. It should be noted that although neglecting wall distensibility may not have a major effect on the primary flow field, the incorporation of wall mechanics in these studies is important for other reasons, including the description of the stress environment within the vessel walls and the interaction between deformability and mass transport phenomena. In summary, the use of rigid models for flow studies in idealized models of the human abdominal aorta should be viewed as a first approximation.

A Newtonian constitutive model for viscosity was used in the present investigation. It is generally accepted that this is a reasonable first approximation to the behavior of blood flow in large arteries. Perktold et al[20] examined non-Newtonian viscosity models for simulating pulsatile flow in carotid artery bifurcation models. They concluded that the shear stress magnitudes predicted with non-Newtonian viscosity models resulted in differences on the order of 10% as compared with Newtonian models. Future studies of abdominal aorta hemodynamic conditions should assess the effects of non-Newtonian rheologic models.

The accuracy of the finite element method for solving the governing equations was not examined quantitatively in the present study because of a lack of published data. In other models, Taylor et al[27] examined the accuracy of this method used for blood flow computations. Numeric results were found to be in excellent agreement with Womersley theory and with laser Doppler anemometry velocity data obtained by Loth[50] for steady and pulsatile flow in a model of an end-to-side anastomosis.[27] It was not possible to examine further refinements in the finite element mesh used as a result of the limitation of computational resources. However, the stabilized finite element method used has been shown to exhibit excellent coarse grid accuracy.[27] It is not expected that further refinements in the mesh will result in substantial qualitative or quantitative differences in the computed solution.

CONCLUSION

The characterization of the temporal and spatial variations of the velocity field in an idealized model of the abdominal aorta enables new insights into the wall shear stresses acting on the luminal surface under resting and exercise conditions. Under resting conditions, regions of low mean wall shear stress and high oscillatory shear index were noted along the anterior wall between the superior mesenteric and inferior mesenteric arteries and along the posterior wall opposite the superior mesenteric artery and approximately 2 cm distal to the renal arteries. Moderate exercise conditions were necessary to eliminate all regions of low mean wall shear stress and high oscillatory shear index. The numeric studies described herein provide further impetus to examine abdominal aorta hemodynamics in vivo with magnetic resonance imaging techniques and to assess the validity of the assumptions made regarding vascular anatomy and physiologic conditions, blood theology, and vessel mechanics.

We thank Jeff Buell, Mary Draney, Alok Mathur, David Parker, and Arthur Raefsky for their assistance. Software was provided by Centric Engineering Systems, Inc, TechnoSoft, Inc, XOX Inc, and Rensselaer Polytechnic Institute's Scientific Computing Research Center. Hewlett-Packard provided a model 755/125 workstation used in this research.

REFERENCES

1. American College of Sports Medicine. Position stand on the recommended quantity and quality of exercise for developing and maintaining cardiorespiratory and muscular fitness in healthy adults. Med Sci Sports Exerc 1990;22:265-74.
2. Pate RR, Pratt M, Blair SN, et al. Physical activity and public health: a recommendation from the Centers for Disease Control and Prevention and the American College of Sports Medicine. JAMA 1995;273:402-7.
3. Blair SN, Kohl HW, Barlow CE, et al. Changes in physical fitness and all-cause mortality: a prospective study of healthy and unhealthy men. JAMA 1995;273:1093-8.
4. Lee I, Hsieh C, Paffenbarger RS. Exercise intensity and longevity in men: the Harvard Alumni Health Study. JAMA 1995;273:1179-84.
5. Fletcher CK, Blair SN, Blumenthal J, et al. AHA medical/scientific statement: statement on exercise. Circulation 1992; 86:340-4.
6. Niebauer J, Cooke JP. Cardiovascular effects of exercise: role of endothelial shear stress. J Am Coll Cardiol 1996;28:1652-60.
7. Pollack ML, Wilmore JH. Exercise in health and disease: evaluation and prescription for prevention and rehabilitation. 2nd ed. Philadelphia: WB Saunders; 1990.
8. Maier SE, Meier D, Boesiger P, Moser UT, Vieli A. Human abdominal aorta: comparative measurements of blood flow with MR Imaging and multigated Doppler US. Radiology 1989;171:487-92.
9. Pedersen EM, Sung HW, Burlson AC, Yoganathan AP. Two-dimensional velocity measurements in a pulsatile flow model of the normal abdominal aorta simulating different hemodynamic conditions. J Biomech 1991;26:10,1237-47.
10. Moore JE, Ku DN, Zarins CK, Glagov S. Pulsatile flow visualization in the abdominal aorta under differing physiologic conditions: implications for increased susceptibility to atherosclerosis. J Biomech Eng 1992;114:391-7.

11. Mostbeck GH, Dulce MC, Caputo GR, Proctor E, Higgins CB. Flow pattern analysis in the abdominal aorta with velocity-encoded cine MR imaging. J Magn Reson Imaging 1993;3:617-23.
12. Bogren HG, Buonocore MH. Blood flow measurements in the aorta and major arteries with MR velocity mapping. J Magn Reson Imaging 1994;4:2,119-30.
13. Moore JE, Maier SE, Ku DN, Boesiger P. Hemodynamics in the abdominal aorta: a comparison of in vitro and in vivo measurements. J Appl Physiol 1994;76:1520-7.
14. Moore JE, Ku DN. Pulsatile velocity measurements in a model of the human abdominal aorta under resting conditions. J Biomech Eng 1994;116:337-46.
15. Moore JE, Xu C, Glagov S, Zarins CK, Ku DN. Fluid wall shear stress measurements in a model of the human abdominal aorta: oscillatory behavior and relationship to atherosclerosis. Atherosclerosis 1994;110:225-40.
16. Moore JE, Ku DN. Pulsatile velocity measurements in a model of the human abdominal aorta under simulated exercise and postprandial conditions. J Biomech Eng 1994;116:107-11.
17. Mohiaddin RH, Gatehouse PD, Firmin DN. Exercise related changes in aortic flow measured with spiral echo-planar MR velocity mapping. J Magn Reson Imaging 1995;5:159-63.
18. Schalet BJ, Taylor CA, Harris EJ, Herfkens RJ, Zarins CK. Quantitative assessment of human aortic blood flow during exercise. Surg Forum 1997;48:359-62.
19. Perktold K, Resch M, Peter R. Three-dimensional numerical analysis of pulsatile flow and wall shear stress in the carotid artery bifurcation. J Biomech 1991;24:6,409-20.
20. Perktold K, Peter RO, Resch M, Langs G. Pulsatile non-Newtonian flow in three-dimensional carotid bifurcation models: a numerical study of flow phenomena under different bifurcation angles. J Biomed Eng 1991;13:507-15.
21. Perktold K, Rappitsch G. Computer simulation of local blood flow and vessel mechanics in a compliant carotid artery bifurcation model. J Biomech 1995;28:7,845-56.
22. Lei M, Kleinstreuer C, Truskey GA. Numerical investigations and prediction of atherogenic—sites in branching arteries. J Biomech Eng 1995;117:350-7.
23. Wells DR, Archie JP Jr, Kleinstreuer C. Effect of carotid artery geometry on the magnitude and distribution of wall shear stress gradients. J Vasc Surg 1996;23:667-78.
24. Lei M, Archie JP, Kleinstreuer C. Computational design of a bypass graft that minimizes wall shear stress gradients in the region of the distal anastomosis. J Vasc Surg 1997;25:637-46.
25. Taylor CA, Tropea BI, Hughes TJR, Zarins CK. Effect of graded exercise on aortic wall shear stress. Surg Forum 1995;46:331-4.
26. Taylor CA, Hughes TJR, Zarins CK. Computational investigations in vascular disease. Comput Phys 1996;10:3,224-32.
27. Taylor CA, Hughes TJR, Zarins CK. Finite element modeling of blood flow in arteries. Comput Methods Appl Mechanics Eng 1998;158:155-96.
28. Taylor CA, Hughes TJR, Zarins CK. Finite element modeling of 3-dimensional pulsatile flow in the abdominal aorta: relevance to atherosclerosis. Ann Biomed Eng 1998;26:6.
29. Shephard MS, Georges MK. Automatic three-dimensional mesh generation by the finite octree technique. Int J Numerical Methods Eng 1991;32:709-49.
30. SHAPES reference manual, XOX, Inc, 1994.
31. Adaptive modeling language theory manual, Technosoft, Inc, 1995.
32. Spectrum theory manual, Centric Engineering Systems, Inc, 1994.
33. Spectrum Visualizer reference manual, Centric Engineering Systems, Inc, 1994.
34. Jorfeldt J, Wahren J. Leg blood flow during exercise in man. Clin Sci 1971;41:459-73.
35. Womersley JR. Method for the calculation of velocity, rate of flow and viscous drag in arteries when the pressure gradient is known. J Physiol 1955;127:553-63.
36. Hughes TJR, Liu WK, Zimmermann TK. Lagrangian-Eulerian finite element formulation for incompressible viscous flows. Comput Methods Appl Mechanics Eng 1981;29:329-49.
37. Hughes TJR. The Finite element method. Englewood Cliffs, NJ: Prentice-Hall; 1987.
38. Brooks AN, Hughes TJR. Streamline upwind Petrov-Galerkin formulation for convection dominated flows with particular emphasis on the incompressible Navier stokes equations. Comput Methods Appl Mechanics Eng 1981; 32:199-259.
39. Hughes TJR, Franca LP, Hulbert GM. A new finite element method for computational fluid dynamics: VIII. The Galerkin/Least Squares method for advective-diffusive equations. Comput Methods Appl Mechanics Eng 1989;73:173-89.
40. Johan Z, Hughes TJR, Shakib F. A globally convergent matrix-free algorithm for implicit time-marching schemes arising in finite element analysis in fluids. Comput Methods Appl Mechanics Eng 1991;87:281-304.
41. Karypis G, Kumar V. A fast and high quality multilevel scheme for partitioning irregular graphs. SIAAA Sci Computing. In press.
42. He X, Ku DN. Pulsatile flow in the human left coronary artery bifurcation: average conditions. J Biomech Eng 1996; 118:74-82.
43. Cornhill JF, Herderick EE, Stary HC. Topography of human aortic sudanophilic lesions. In: Liepsch DW, editor. Blood flow in large arteries: applications to atherogenesis and clinical medicine. Basel, Switzerland: Karger; 1990. p. 13-19.
44. Caro CG, Doorly DJ, Tamawski M, Scott KT, Long Q, Dumoulin CL. Non-planar curvature and branching of arteries and non-planar type flow. Proc R Soc 1996;452:185-97.
45. Zarins CK, Giddens DP, Bharadvaj BK, Sottiurai VS, Mabon RF, Glagov S. Carotid bifurcation atherosclerosis: quantitative correlation of plaque localization with flow velocity profiles and wall shear stress. Circ Res 1983;53:502-14.
46. Ku DN, Giddens DP, Zarins CK, Glagov S. Pulsatile flow and atherosclerosis in the human carotid bifurcation. Positive correlation between plaque location and low oscillating shear stress. Arteriosclerosis 1985;5:293-302.
47. Zarins CK, Taylor CA. Hemodynamic factors in atherosclerosis. In: Moore W, editor. Vascular surgery: a comprehensive review. 5th ed. Philadelphia: WB Saunders Co; 1998. p. 97-110.
48. Holenstein R, Ku DN. Reverse flow in the major infrarenal vessels—a capacitive phenomenon. Biorheology 1988;25:835-42.
49. Pelc NJ, Sommer FG, Li KCP, Brosnan TJ, Herfkens RJ, Enzmann DR. Quantitative magnetic resonance flow imaging. Magn Reson Q 1994;10:3,125-47.
50. Loth F. Velocity and wall shear stress measurements inside a vascular graft model under steady and pulsatile flow conditions [dissertation]. Atlanta: Georgia Institute of Technology, 1993.

Submitted Sep 16, 1998; accepted Dec 11, 1998.